DIGITAL WAVEGUIDE MESH MODELLING OF ROOM ACOUSTICS: IMPROVED ANECHOIC BOUNDARIES

Damian T. Murphy and Jack Mullen

Department of Electronics
University of York, Heslington, York, YO10 5DD, UK
dtm3@ohm.york.ac.uk

ABSTRACT

Digital waveguide mesh structures have proved useful in a wide variety of modelling applications. When modelling the acoustics of an enclosed space the accurate simulation of specific boundary conditions is paramount but waveguide mesh related techniques have as yet to provide an appropriate and reliable solution. This paper gives an overview of boundary types that have been implemented by researchers to date and describes the application of a higher order approximation for the particular case of an anechoic boundary, that may prove useful as part of a more general solution.

1. INTRODUCTION

When modelling the acoustic properties of a room geometrical algorithms such as ray-tracing [1] or the image-source method [2] are often used. Alternative methods implement scattering algorithms to model physical wave propagation and can be shown to demonstrate typical wave phenomena such as diffraction and interference that cannot be accounted for in a geometrical solution. Scattering algorithms as implemented using a digital waveguide mesh model have provided an accurate and efficient method of physically modelling 2D and 3D resonant systems such as membranes and plates [3], drums [4] and rooms [5].

This work is particularly interested in using digital waveguide mesh structures for reverberation and room acoustics modelling, these being fundamental tools in the field of creative audio processing. The aim is to arrive at an accurate room impulse response (RIR) measurement for the modelled space that can then be used in a convolution operation with an arbitrary audio input. As such the characteristics of the room will be imparted onto the audio signal, effectively placing the listener within the modelled space. Despite some of the shortcomings of the waveguide mesh technique the results obtained are encouraging although they are let down in terms of their overall quality by poorly implemented boundary conditions. This also means that it is difficult to compare the results with actual real world RIR measurements to see how successful these models actually are. The boundaries in a room are a primary feature that help to determine its reverberant characteristics and how it will affect the timbre of an audio event (musical or otherwise) heard within its confines. Smooth, flat walls usually impart a bright or cold characteristic to the source material, with a longer decay. Softer materials give a sense of warmth, and the increased absorption shortens the reverberation time. These boundaries are also invariably frequency dependent. In geometrical or generic filter based reverb algorithms, the effects of a boundary can be easily implemented or changed use variable delay lines and combinations of high-pass/low-pass filters. In a physical model such as the digital waveguide mesh a more considered analytical approach has to be taken.

This paper gives an overview of the methods that have been used to date to implement accurate boundaries as part of a digital waveguide mesh structure, with their associated advantages and limitations. It then goes on to look at the particular problem of accurately modelling an anechoic boundary and how current implementations can be improved by using a higher order solution.

2. THE DIGITAL WAVEGUIDE MESH

A waveguide is any medium in which wave motion can be characterised by the one-dimensional wave equation. In the lossless case, all solutions can be expressed in terms of left-going and right-going travelling waves and can be simulated using a bi-directional digital delay line. A digital waveguide model is obtained by sampling, both in space and time, the one-directional travelling waves occurring in a system of ideal lossless waveguides [6]. The sampling points in this case are called scattering junctions, and are connected by bi-directional unit-delay digital waveguides [7]. Figure 1(a) shows the general case of a scattering junction J with N neighbours, $i = 1,2,\ldots N$.

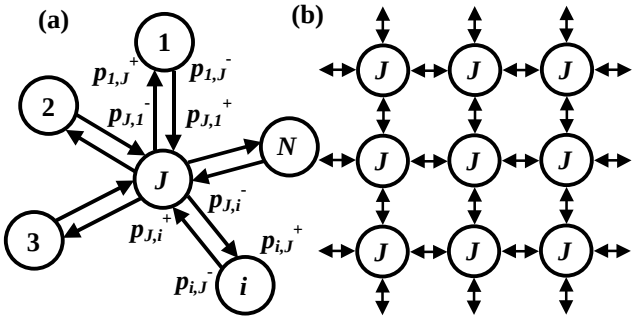

Figure 1: *(a) A general scattering junction J with N connected waveguides for i = 1,2,…,N; (b) 2D rectilinear mesh structure.*

The sound pressure in a waveguide is represented by p_i, the volume velocity by v_i and the impedance of the waveguide by Z_i. The input to a waveguide is termed p_i^+ and the output p_i^-. The

signal $p_{i,J}^{+}$ therefore represents the incoming signal to junction i along the waveguide from the opposite junction J. Similarly, the signal $p_{i,J}^{-}$ represents the outgoing signal from junction i along the waveguide to the opposite junction J. The volume velocity v_i is equal to pressure, p_i, divided by impedance, Z_i. The delay elements are bi-directional and so the sound pressure is defined as the sum of its input and output:

$$p_i = p_i^{+} + p_i^{-} \qquad (1)$$

At a lossless scattering junction with N connected waveguides the following conditions must hold:

1. The sum of the input volume velocities, v^{+}, equals the sum of the output volume velocites, v^{-}:

$$\sum_{i=1}^{N} v_i^{+} = \sum_{i=1}^{N} v_i^{-} \qquad (2)$$

2. The sound pressures in all crossing waveguides are equal at the junction:

$$p_1 = p_2 = ... = p_i = ... = p_N \qquad (3)$$

Using these conditions the sound pressure at a scattering junction can be expressed as:

$$p_J = \frac{2\sum_{i=1}^{N} \frac{p_i^{+}}{Z_i}}{\sum_{i=1}^{N} \frac{1}{Z_i}} \qquad (4)$$

As the waveguides are equivalent to bi-directional unit-delay lines, the input to a scattering junction is equal to the output from a neighbouring junction into the connecting waveguide at the previous time step. This can be expressed as:

$$p_{J,i}^{+} = z^{-1} p_{i,J}^{-} \qquad (5)$$

Note that using equations (1), (4) and (5) it is also possible to derive an equivalent finite difference formulation for these scattering equations in terms of junction pressure values only:

$$p_J(n) = \frac{1}{2}\sum_{i=1}^{4} p_i(n-1) - p_J(n-2) \qquad (6)$$

Where equation (6) is the finite difference formulation of the scattering equations for a 4-port waveguide structure with equal impedances.

By discretising the 2D plane, rectilinear and triangular mesh structures can be constructed using unit delay waveguides and lossless scattering junctions with N = 4 and N = 6 in Equation 4 respectively, forming a 2D medium that can sustain wave propagation. Figure 1(b) shows the 2D rectilinear waveguide mesh with N = 4. A signal representing acoustic pressure introduced to a waveguide will propagate in either direction along the bi-directional delay lines until it comes to a junction. The signal then scatters according to the relative impedances of the connected waveguides. In the current model, as in Equation (6), all impedances are set to be equal.

Wave propagation through the rectilinear mesh (as shown in Figure 2) has been shown to exhibit direction and frequency dependant dispersion [6]. This leads to wave propagation errors and mis-tuning of the expected resonant modes for a 2D or 3D structure. Solutions have been proposed to minimise this dispersion error, two of which use alternative triangular [8] or bilinearly deinterpolated rectilinear mesh topologies [9].

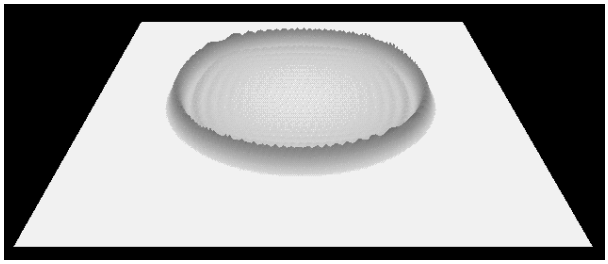

Figure 2. *Wave propagation on the 2-D Rectilinear Digital Waveguide Mesh.*

3. BOUNDARY MODELLING

At the boundary of a mesh structure an interaction occurs between the terminating junction (usually at or on the boundary itself) and its immediate neighbour (within the main body of the mesh structure). In general, a boundary junction is defined as having only one other neighbour - interaction is only allowed between the boundary junction and junctions within the mesh, with adjacent junctions lying on the boundary having no direct influence on each other. The effect of a boundary in a real room is to produce a reflection of an incident sound wave, usually with some frequency dependent absorption of the wave energy at the boundary itself. In a digital waveguide structure a reflection is caused by a change in the impedance of the waveguide. This can be conceptualised by connecting a dummy junction on the other side of the boundary junction, essentially within the boundary itself, as in Figure 3. The connecting waveguides on either side of the boundary will have different characteristic impedances, Z_1 and Z_2 respectively.

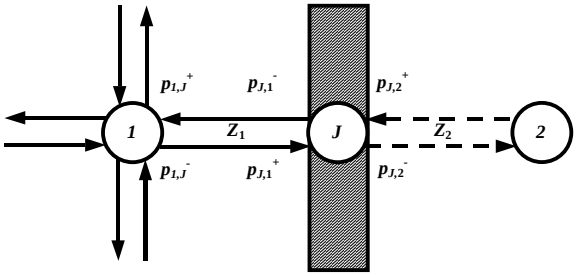

Figure 3: *Termination of a waveguide mesh due to a boundary resulting in a reflection.*

If at a boundary the impedance changes from Z_1 to Z_2 the reflection coefficient r is defined as:

$$r = \frac{Z_2 - Z_1}{Z_2 + Z_1} \qquad (7)$$

Given that there is no contribution into the boundary junction, J, from the dummy junction 2 and using (4) and (5), the sound pressure for the boundary junction can be calculated as a function of the sound pressures of the incident travelling waves, p_i^{+} giving:

$$p_J = (1+r)\cdot p_{J,1}^{+} \qquad (8)$$

Or, in an equivalent finite difference formulation:

$$p_J = (1+r)\cdot p_1(n-1) - r\cdot p_J(n-2) \qquad (9)$$

In general, simple absorption can be modelled at such a boundary by replacing the junction adjacent to the boundary itself with the equivalent *n*-port junction (where n = 1,2,…,5 for a triangular mesh), according to the room/boundary geometry that the mesh model has to fit. The amount of energy reflected at the boundary is determined by setting r equal to a value between 0 and 1. With r = 0 boundary nodes assume the value of their neighbour (free end) and anechoic conditions are simulated. With r = 1 a phase preserving total reflection with no absorption is simulated. Additionally, setting r = -1 effectively fixes the boundary junction to zero and results in phase reversing reflection.

Although these boundary conditions are satisfactory in most cases they are clearly an oversimplification of reality even though they are consistent with mesh construction and offer a solution that enables simple reflection and absorption to be modelled. This non-ideal behaviour is most clearly evidenced when modelling anechoic conditions, where significant reflections at high frequencies can be seen [10], [5]. Additionally, real acoustic boundaries are both frequency and direction dependent and this has not been considered in the derivation of the boundary conditions.

3.1. More Accurate Boundary Implementations

Using the derivation of a boundary for a digital waveguide mesh as discussed above as a starting point, a number of improvements have been suggested. In [11], the boundary junction in Figure 4 is replaced with a boundary filter with transfer function *H(z)*. This transfer function is defined to optimally match given frequency dependent reflection coefficient data for a particular material, and implemented using a first order IIR filter. The results given are a good approximation to the required target responses, but are again subject to the directional dependent characteristics of the mesh structure itself, being less accurate for certain angles of incidence.

For curved boundaries, where the perimeter of the structure being modelled (such as a drum membrane) in not normal/parallel to the axes of the mesh structure, *rimguides* have been suggested as an appropriate solution [12]. Rimguides are non-integer length waveguide elements, comprising an integer length waveguide and a first order all-pass filter to model the fractional part. This method has been shown to be accurate for modelling circular membranes using a triangular mesh at low frequencies where the time for a wave to travel diametrically across the model is the same as it would be in a real membrane. The model becomes less accurate with increasing frequency, although this is most likely due to the frequency dependent dispersion characteristics of the triangular mesh.

This method has been extended to model the effect of diffuse reflections at a boundary [13]. At a smooth boundary the angle of incidence is equal to the angle of reflection, resulting in *specular* reflections. At an irregular surface a *diffuse* reflection is produced where energy is scattered in almost every direction regardless of the angle of incidence. This is a very important property in room acoustics as very few surfaces act to produce perfectly specular reflections. A diffuse boundary has been implemented by using circulant matrices to rotate and pre-alter the angle of incidence of a wavefront by a random amount, scattering energy in many directions regardless of initial angle of incidence. This is achieved by multiplying the incoming signals to a junction adjacent to the boundary of the mesh with a circulant matrix designed to ensure that the signal strength and power of the wavefront is conserved. The effect of this matrix transformation is to rotate the incident wave about the junction it is applied. This rotation is then randomly altered for each time step to achieve the diffusion effect. The amount of diffusion applied can be varied as required by changing this angle of rotation. Diffuse boundaries have been applied with some success to a small circular mesh based on a triangular topology using rimguides to connect the mesh to the required boundary. It has been suggested that it should be a small step to implement a frequency dependent variation on this design by replacing the coefficients within the circulant matrix with appropriately designed filters.

4. ANECHOIC BOUNDARIES

An indication of the behaviour of a particular mesh structure and its associated boundaries can be obtained by attempting to model anechoic conditions, as all propagating wave energy within the mesh should be absorbed as it arrives at the boundary. An ideal anechoic boundary (either the actual physical material or the computationally modelled equivalent) is designed to simulate free-field radiation such that the acoustic medium extends to infinity, being ideally transparent to all incident acoustic waves. This is simulated in an anechoic chamber by using an alternating arrangement of absorbent wedges mounted on the interior surfaces as shown in Figure 4. The wedge shape is designed to absorb all echoes or reflections by acting as a waveguide such that all incident acoustic energy is internally reflected into the wedge and its neighbours. The alternating pattern is used to give more uniform angular absorption.

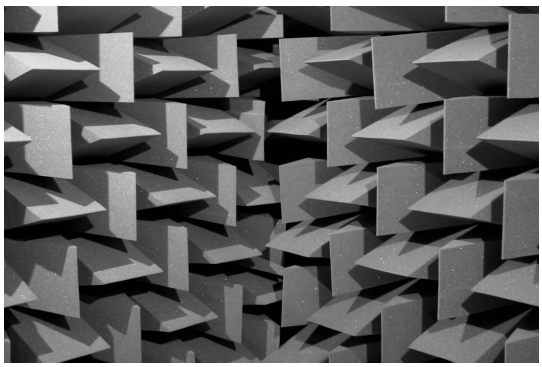

Figure 4: *The Music Technology Group at York's Anechoic Chamber showing the alternating arrangement of absorbing wedges.*

Clearly it is impractical to model an anechoic boundary numerically along the same lines as they are constructed

physically. Rather a domain must be defined such that numerical wave propagation in all directions can be modelled successfully (in this case the actual digital waveguide mesh), together with a boundary condition that permits outward propagation of this simulated wave as if the interior computational domain was of an infinite extent. This boundary must also suppress spurious reflections of the outgoing wave, something which currently implemented boundaries are not capable of achieving [10]. Considerable effort has been spent examining this problem in computational electrodynamics [14] and these types of boundary conditions are generally termed Absorbing Boundary Conditions (ABCs). Problems in this area usually make use of a finite difference algorithmic solution for Maxwell's curl equations in the interior domain. As the digital waveguide mesh has an equivalent finite difference formulation it is appropriate to look for suitable ABC solutions from this related subject area. One such method used in an acoustics context, makes use of a Taylor's series expansion about the boundary junction, and has been successfully implemented to model the open end of the vocal tract [15].

4.1. The Taylor Series ABC

Consider a boundary junction p_B and a stencil of pressure values $p_i(t\text{-}i+1)$ for junctions positions p_i along a straight line perpendicular to this boundary, being both equidistant in time and space, as shown in Figure 5.

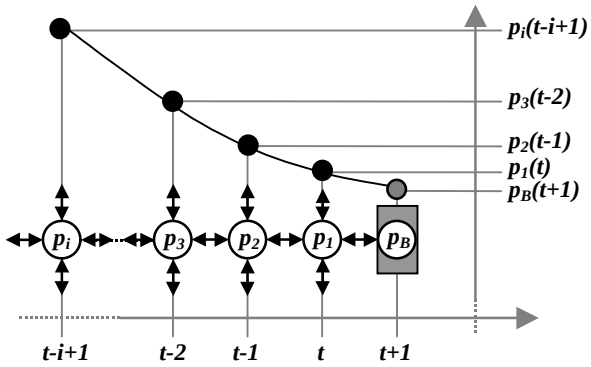

Figure 5: *Boundary junction p_B and connected junctions p_i with associated pressure values $p_i(t\text{-}i+1)$ used in a Taylor Series approximation for junction value $p_B(t+1)$.*

An approximation for the updated junction value, $p_B(t+\Delta t)$, is required. Note that in Figure 5, as in the waveguide mesh algorithm, it is assumed $\Delta t = 1$. Therefore we define the following values:

$$\begin{aligned} P_B &= p_B(t+1) \\ P_1 &= p_1(t) \\ P_2 &= p_2(t-1) \\ P_3 &= p_3(t-2) \\ P_i &= p_i(t-i+1) \end{aligned} \qquad (10)$$

Together with the associated sequence of backward differences originating at P_1:

$$\begin{aligned} \nabla^1 P_1 &= P_1 - P_2 \\ \nabla^2 P_1 &= \nabla^1 P_1 - \nabla^1 P_2 \\ \nabla^3 P_1 &= \nabla^2 P_1 - \nabla^2 P_2 \end{aligned} \qquad (11)$$

Assuming that the function defined by these points is continuous, and as the value $p_1(t)$ is known (as it is calculated within the domain of the mesh) then it is possible to approximate the point $p_B(t+1)$ as a Taylor series expansion about the point $p_1(t)$ with $h = \Delta t = 1$ as follows:

$$p_B(t+1) = p_1(t) + \Delta t p'_1(t) + \frac{\Delta t^2}{2!} p''_1(t) + \frac{\Delta t^3}{3!} p'''_3(t) + \ldots$$

$$\Rightarrow p_B(t+1) = p_1(t) + \nabla^1 P_1 + \frac{1}{2}\nabla^2 P_1 + \frac{1}{6}\nabla^3 P_1 + \ldots \quad (12)$$

Using this Taylor series expression together with equations (10) and (11) it is therefore possible to derive the pressure value at p_B in terms of the pressure values p_i for time $t = t+1$ with increasing orders of accuracy as follows:

$$p_B(t+1)_0 = p_1(t) \qquad (13)$$

$$\begin{aligned} p_B(t+1)_1 &= p_B(t+1)_0 + \nabla^1 P_1 \\ &= 2p_1(t) - p_2(t-1) \end{aligned} \qquad (14)$$

$$\begin{aligned} p_B(t+1)_2 &= p_B(t+1)_1 + \tfrac{1}{2}\nabla^2 P_1 \\ &= \tfrac{5}{2} p_1(t) - 2p_2(t-1) + \tfrac{1}{2} p_3(t-2) \end{aligned} \qquad (15)$$

$$\begin{aligned} p_B(t+1)_3 &= p_B(t+1)_2 + \tfrac{1}{6}\nabla^3 P_1 \\ &= \tfrac{8}{3} p_1(t) - \tfrac{5}{2} p_2(t-1) + p_3(t-2) - \tfrac{1}{6} p_4(t-3) \end{aligned} \qquad (16)$$

Note that Equation (13), the zero order term, is equivalent to Equation (9) with $r = 0$, being the currently implemented anechoic boundary and as such it is clear that there would be considerable error with this boundary implementation that should be improved by using a higher order solution.

5. RESULTS

A 100x100 junction 2D rectilinear mesh has been constructed and a smooth gaussian impulse has been applied as an input over four time steps at junction (50,70) of this mesh. All boundaries are defined as being equivalent and have been implemented using each of the successively more accurate anechoic boundary solutions presented in Equations (13)-(16). Impulse response measurements have been made at junctions (50,100) and (50,85). The first case being one of the anechoic boundary junctions, and the second being just away from this same point in a perpendicular direction, within the actual mesh domain. Care was taken to ensure that boundaries not being examined were at an appropriate relative distance from the measurement point to avoid additional reflections influencing the results.

Figure 6 displays the measured impulse responses, with 6(a) being the results for junction (50,100) (on boundary) and 6(b) being the results for junction (50,85) (off boundary). Note that in both cases the two plots shown in each graph are for the zero

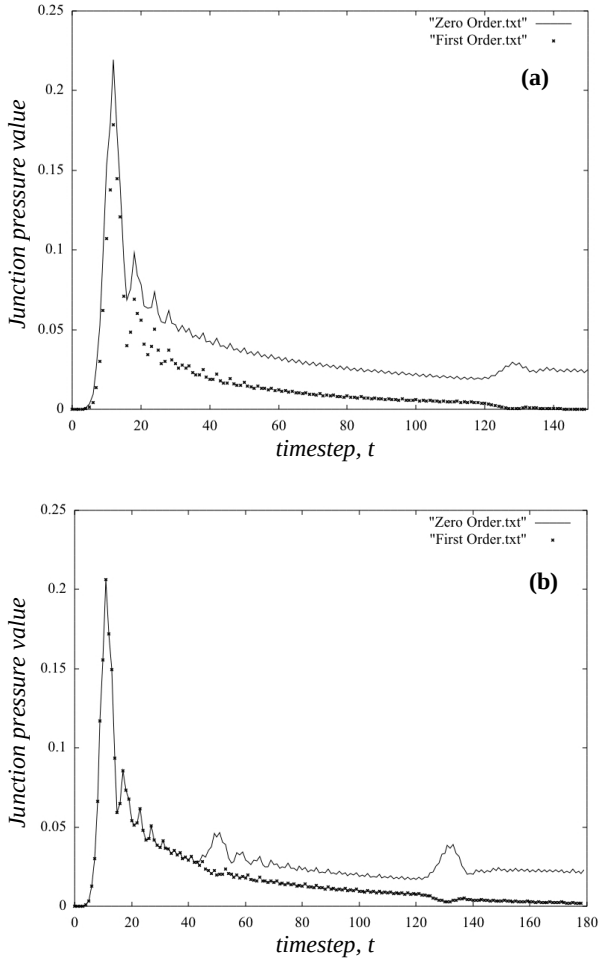

Figure 6: *Impulse response measurements demonstrating the Taylor series formulation of an anechoic boundary junction with zero order (solid lines) and first order (dotted lines) results plotted. (a) For a junction on the boundary itself; (b) for a junction within the mesh, being close to the actual boundary.*

order case (Equation (13)), represented by the solid line, and the first order case (Equation (14)), represented by the dotted line, only.

Figure 6(a) demonstrates the significantly improved absorption characteristics of the first order boundary over the standard zero order implementation. Once the incident wave has arrived at the boundary junction the energy has effectively dissipated by time t = 120 whereas in the zero order case the boundary junction has as yet to return to rest. Figure 6(b) demonstrates how the boundaries act to suppress reflected components generated as the incident wave passes "through" the boundary. Note that distinct reflections can be evidenced at times t = 50 and t = 130 for the zero order boundary that are not apparent for the first order case. The first reflection has been generated from the boundary actually being tested with the second being the constructive sum of the two reflections from the two adjacent side boundaries.

Note that despite implementing Taylor series anechoic boundaries of this type up to third order, no discernable improvement in accuracy can be evidenced when the results are plotted, with almost identical impulse responses being produced. When the actual numerical results are investigated the differences between first, second and third order become apparent, but this improvement is insignificant when compared with the relative measured difference between the results for zero and first order boundaries. This is beneficial from an implementation perspective as the model is more efficient in terms of boundary computation and total memory requirements. Note that for boundaries above second order, additional mesh history is required, beyond that of the two previous time steps needed to implement the standard 2D rectilinear junction within the actual mesh domain. However, the slight improvement that is offered by higher order solutions may be significant for the modelling scheme as a whole and as such a more considered error analysis is required, together with a high sample rate implementation suitable for audio processing purposes to investigate any possibly related perceptual effects.

6. CONCLUSIONS

An anechoic ABC based on a Taylor series approximation of the pressure value at a junction on a boundary of a simple 2D rectilinear digital waveguide mesh has been derived and tested. The zero order approximation has been shown to be equivalent to the standard waveguide mesh implementation of an anechoic boundary based on a change of impedance in the mesh structure. The first order approximation has been shown to offer a significant improvement over this zero order case, demonstrating a much higher absorption of incident wave energy together with the successful suppression of additional spurious reflections from the boundary itself. Second and third order approximations do not seem to offer any significant improvement on the first order case based on the impulse response measurements obtained, although analysis of the numerical data shows some slight improvement may be evident that is worthy of further investigation. Therefore, it would seem that the first order approximation is the most applicable implementation of an anechoic ABC offering improved performance with low computational overhead.

From a room acoustics modelling perspective, an accurate anechoic ABC is of limited use. However this work has a number of advantages within the field of digital waveguide mesh modelling. Clearly there are parallels with the comparable fields of finite difference and transmission line modelling, and this study shows that boundary solutions as implemented for these similar algorithms can be applied with some success in a digital waveguide mesh. This would therefore indicate that other similar boundary models might be worth investigating further. Currently the state of the art in computational electromagnetics is the *Berenger Perfectly Matched Layer* ABC [14] although it is not obvious how this might be applied in an acoustics context. In addition, a numerical approximation, having been successful in this particular case, may prove to be a valid approach for modelling a general boundary junction with more realistic reflection/absorption characteristics. Finally, if a more complex real-world boundary is to be simulated and tested, accurately

modelled anechoic conditions at boundaries on the mesh other than that under investigation will ensure the results will be free from the influence of reflections from other non-critical sources.

Future work will involve a more comprehensive investigation and error analysis of the higher order boundary conditions, together with an examination of audio examples produced from mesh structures subject to these conditions for evidence of any related effects. Work is already under way on the implementation of this anechoic ABC for both the triangular and bilinearly deinterpolated mesh topologies, as both of these structures offer significant improvements in terms of dispersion error and wave propagation characteristics over the rectilinear mesh. A broader study will look at how this anechoic ABC might be extended to the more general case and examine how other potentially promising boundary modelling solutions might be successfully implemented for a digital waveguide mesh structure.

7. REFERENCES

[1] Krokstad A., Strøm S., and Srøsdal, S., "Calculating the Acoustical Room Response by use of a Ray Tracing Technique", *Journal of Sound Vibration*, Vol. 8, No. 1, pp 118-125, 1968.

[2] Stephenson, U., "Comparison of the Mirror Image Source Method and the Sound Particle Simulation Method", *Applied Acoustics*, Vol. 29, pp 35-72, 1990.

[3] Fontana, F., and Rocchesso, D., "A New Formulation of the 2D-Waveguide Mesh for Percussion Instruments", *Proceedings of the XI Colloquium on Musical Informatics*, pp. 27-30, Bologna, Italy, November 1995.

[4] Aird, M., Laird, J., and Fitch, J., "Modelling a drum by interfacing 2D and 3D waveguide meshes", *Proceedings of the International Computer Music Conference*, Berlin, Germany, 2000.

[5] Savioja, L., Rinne, T. J., and Takala, T., "Simulation of Room Acoustics with a 3-D Finite Difference Mesh", *Proceedings of the International Computer Music Conference*, pp. 463-466, Denmark, 1994.

[6] Van Duyne, S. A. and Smith, J. O., "Physical Modeling with the 2-D Digital Waveguide Mesh", *Proceedings of the International Computer Music Conference*, pp. 40-47, Tokyo, Japan, 1993.

[7] Smith, J. O., "Physical modelling using digital waveguides", *Computer Music Journal*, Vol. 16, No. 4, pp. 74-87, Winter 1992.

[8] Murphy, D.T., and Howard, D. M., "2-D Digital Waveguide Mesh Topologies in Room Acoustics Modelling", *Proceedings of the Cost G-6 Conference on Digital Audio Effects (DAFX-00)*, pp. 211-216, Verona, Italy, Dec. 7-9, 2000.

[9] Savioja, L., and Välimäki, V., "Reducing the Dispersion Error in the Digital Waveguide Mesh Using Interpolation and Frequency-Warping Techniques", *IEEE Trans. Speech and Audio Process*ing, Vol. 8, pp. 184-194, 2000.

[10] Murphy, D. T., Newton, C. J. C., and Howard, D. M., "Digital Waveguide Mesh Modelling of Room Acoustics: Surround-sound, Boundaries and Plugin Implementation", *Proceedings of the Cost G-6 Conference on Digital Audio Effects (DAFX-01)*, pp. 198-202, Limerick, Ireland, Dec. 6-8, 2001.

[11] Huopaniemi, J., L. Savioja, L., and Karjalainen, M., "Modelling of Reflections and Air Absorption in Acoustical Spaces – A Digital Filter Design Approach", *Proceedings of the 1997 IEEE Workshop on Applications of Signal Processing to Audio and Acoustics (WASPAA'97)*, Mohonk Mountain House, New Paltz, New York, Oct. 19-22,1997.

[12] Laird, J., Masri, P., and Canagarajah, C. N., "Efficient and Accurate Synthesis of Circular Membranes Using Digital Waveguides", *Proceedings of the IEE Colloquium on Audio and music technology: The creative challenge of DSP*, IEE Digest 98/470, pp. 12/1-12/6, 1998.

[13] Laird, J., Masri, P., and Canagarajah, N., "Modelling Diffusion at the Boundary of a Digital Waveguide Mesh", P*roc. ICMC*, pp 492-495, China, 1999.

[14] Tavlove, A., "Computational Electrodynamics: The Finite Difference Time-Domain Method", Artech House, Boston, 1995.

[15] El-Masri, S., Perolson, X., Saguet, P., and Badin, P., "Vocal Tract Acoustics Using the TLM Method", *Proceedings of the International Conference on Speech and Language Processing*, Vol. 2, pp. 953-956, 1996.